High-Performance Fiber-Reinforced Concrete Coupled-Wall Systems: Design and Behavior

R. D. Lequesne
University of Michigan, Ann Arbor, MI, USA

J. K. Wight
University of Michigan, Ann Arbor, MI, USA

G. J. Parra-Montesinos
University of Michigan, Ann Arbor, MI, USA

ABSTRACT:
Two large-scale, four-story, coupled-wall specimens were tested under lateral displacement reversals to investigate the use of strain-hardening, high-performance fiber-reinforced concrete (HPFRC) in critical regions of coupled-wall systems. Each specimen consisted of four precast HPFRC and reinforced concrete coupling beams, with span-to-height ratios of 1.75, which linked two T-shaped structural walls. In the first specimen, the wall was constructed with regular concrete and designed according to the 2008 ACI Code. The lower two stories of the second coupled-wall were constructed with HPFRC and simplified reinforcement detailing.

A stable response with high energy dissipation was achieved for both specimens, resulting in a highly damage tolerant system. Both specimens exhibited a predictable strength and excellent behavior up to wall drift levels of approximately 3%. The HPFRC enhanced the shear capacity of the beams and provided confinement to the diagonal reinforcement, permitting a 50% reduction of the diagonal reinforcement area and a 60% reduction of the transverse reinforcement. The use of HPFRC in the second coupled-wall allowed for a reduction of transverse reinforcement for confinement and a higher concrete contribution to shear strength.

Keywords: seismic design, coupling beam, coupled-wall system, HPFRC

1. INTRODUCTION

For satisfactory performance of a coupled-wall system during a seismic event, coupling beams, typically with aspect ratios less than 3.5, must retain a significant strength and stiffness through large displacement reversals. To ensure that adequate coupling beam ductility is achieved, the ACI Building Code (ACI 318-08) requires the use of diagonal reinforcement to resist all of the shear demand in short and highly stressed coupling beams. This reinforcement detail has been shown by many researchers to provide a stable behavior under earthquake-type displacement reversals, but can be difficult and time consuming to construct. Results from recent coupling beam component tests (Canbolat, Parra-Montesinos and Wight 2005, Lequesne et al. 2009) have demonstrated that precasting coupling beams with strain-hardening HPFRC can simplify the construction process without sacrificing overall performance. In addition to relaxing the reinforcement requirements for coupling beams, HPFRC can simplify the detailing in the critical lower stories of structural walls because of its improved ductility and contribution to shear resistance and confinement of the longitudinal reinforcement.

2. RESEARCH SIGNIFICANCE

An experimental investigation of the impact of using precast HPFRC coupling beams on the design, constructability, and seismic performance of coupled walls is presented. This paper discusses: 1) an evaluation of the effectiveness of combining HPFRC and reduced boundary element confinement in plastic hinge regions of structural walls, 2) a comparison of the behavior of HPFRC and RC coupling beams subjected to similar deformation demands, and 3) observations of the interaction between HPFRC coupling beams, slabs, and structural walls.

3. MATERIAL PROPERTIES

The HPFRC mixture design used for this study, developed by Liao et al. (2006), is shown in Table 3.1. It includes a 1.5% volume fraction (v_f) of high-strength hooked steel fibers (see Table 3.2 for fiber properties), and coarse aggregate with a maximum nominal size of 0.5 in. (13 mm). The conventional concrete used throughout this study was either mixed in the laboratory or delivered by local suppliers, and had a specified compressive strength (f_c') of 6 ksi (41 MPa).

Table 3.1. Concrete matrix proportions by weight of cement

Cement (Type III)	Fly Ash	Sand	Aggregate	Water	Superplasticizer	Viscosity Modifying Agent
1	0.88	2.2	1.2	0.8	0.005	0.038

Table 3.2. High-strength hooked steel-fiber properties

Length (in. / mm)	Diameter (in. / mm)	L/d	Specified Tensile Strength (ksi / MPa)
1.2 / 30	0.015 / 0.38	80	333 / 2300

Table 3.3. Concrete properties

	Portion of Specimen	Fiber Y/N	28-Day Tests					Test Day f'_c (ksi / MPa)
			f'_c (ksi / MPa)	ASTM 1609 Flexural Tests (psi / MPa)				
				σ_{fc} [a]	σ_{peak} [b]	$\sigma_{(\delta=L/600)}$ [c]	$\sigma_{(\delta=L/150)}$ [d]	
CW-1	CB-1 & CB-3	Y	5.5 / 38	710/ 4.9	1030 / 7.1	970 / 6.7	520 / 3.6	10.3 / 71
	CB-2	N	5.3 / 37					9.8 / 68
	CB-4	Y	6.0 / 41	830 / 5.7	1120 / 7.7	1050 / 7.2	600 / 4.1	10.8 / 74
	Wall 1st lift	N	5.3 / 37					7.0 / 48
	Wall 2nd lift	N	4.1 / 28					6.7 / 46
CW-2	CB-1 & CB-4	Y	6.0 / 41	830 / 5.7	1120 / 7.7	1050 / 7.2	600 / 4.1	10.4 / 72
	CB-2	N	6.6 / 46					9.2 / 63
	CB-3	Y	5.5 / 38	710 / 4.9	1030 / 7.1	970 / 6.7	520 / 3.6	10.4 / 72
	Wall 1st lift	Y	2.7 / 19					2.7 / 19
	Wall 2nd lift	Y	6.7 / 46	835 / 5.8	1050 / 7.2	1010 / 7.0	570 / 3.9	7.3 / 50

[a] Peak bending stress at first cracking
[b] Equivalent bending stress at peak stress
CW: coupled wall (1 lift = 1 wall story)
[c] Equivalent bending stress at a deflection of L/600
[d] Equivalent bending stress at a deflection of L/150
CB: coupling beam (see Fig. 4.4)

Table 3.4. Mild steel reinforcement properties

Specimen	Bar Size (US / mm)	Yield Stress (ksi / MPa)	Ultimate Stress (ksi / MPa)
Coupled Walls	#6 / 19	64.2 / 440	108 / 745
	#5 / 16	67.2 / 465	109 / 750
	#4 / 13	60.1 / 415	97.0 / 670
	#3 / 10 (CW-1)	71.8 / 495	112 / 770
	#3 / 10 (CW-2)	67.3 / 465	117 / 805
	#2 / 6	64.1 / 440	73.3 / 505
Coupling Beams	#4 / 13	75.7 / 520	116 / 800
	#3 / 10	71.1 / 490	114 / 785
	#2 / 6	64.1 / 440	73.3 / 505

Results from compressive tests of 4 in. by 8 in. (100 mm by 200 mm) cylinders and four-point bending tests performed in accordance with ASTM C1609–05, are shown in Table 3.3. The results from these bending tests showed pronounced deflection hardening behavior, with peak bending stresses that exceeded the first cracking stress by more than 30% near deflections of L/800, where L is the beam span length (18 in. or 450 mm). Results from tests on representative coupons of the reinforcing steel used in this study are listed in Table 3.4.

4. COUPLED-WALL SYSTEM TESTS

Two four-story coupled wall specimens were built at approximately one-third scale and subjected to earthquake-type lateral displacement reversals. A completed specimen and testing setup is shown in Fig. 4.1. Lateral displacements were pseudo-statically applied through the slabs cast at the second and fourth levels. The actuator mounted on the fourth level applied a predetermined sequence of reversing lateral displacements, while the actuator at the second level applied a force equivalent to 60% of the force applied by the top actuator. These lateral forces were transferred to the coupled walls through a yolk and four channel sections that were attached to the top and bottom of the outer edges of the slabs. This was intended to allow for a distribution of lateral force to each of the structural walls that is similar to the load transfer mechanism that develops in a real building system. The slabs also provided an opportunity to observe the interaction between precast coupling beams and the adjacent slab, and to evaluate the need for design modifications to minimize damage at this interface.

The base of each wall was embedded in deep reinforced concrete foundation elements bolted directly to the laboratory strong floor. A vertical force, equivalent to an axial stress of 7% of the specified f_c', based on the gross area of the walls, was applied at the second story through external prestressing tendons anchored at the bottom of the foundation. Steel tube sections embedded through each wall above the second story slab transferred force from the external tendons into the walls. Hydraulic jacks were used to apply this vertical force before any lateral displacement was applied. The vertical force was held constant throughout the test. This level of gravity load is consistent with current design practice for structural walls and was sufficient to offset a majority of the uplift force resulting from the coupling of the walls.

Figure 4.1. Photo of test specimen

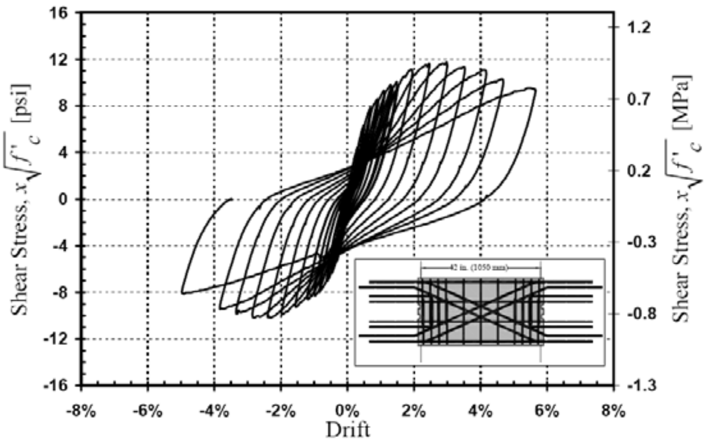

Figure 4.2. Shear stress vs. drift for HPFRC coupling beam

4.1. HPFRC Coupling Beams

The general design approach for the coupling beams used in the coupled-wall tests was developed through two series of tests on HPFRC coupling beam components (Canbolat, Parra-Montesinos, and Wight 2005, Lequesne et al. 2009). A sample hysteresis behavior from the most recent series of tests of large-scale, precast HPFRC coupling beams with span-to-depth ratios (l_n/h) of 1.75 is shown in Fig. 4.2. The results indicate that HPFRC contributes appreciably to the shear capacity of the coupling beam, provides confinement to diagonal reinforcement, and results in improved damage tolerance evidenced by reduced crack widths and wide shear force vs. member drift hysteresis loops. A method of precasting and embedding the coupling beam into the adjacent walls, without interrupting the wall boundary reinforcement, was also developed and shown to successfully force flexural rotations to localize away from the beam-wall interface.

Typical reinforcement details used in the coupling beams of the coupled-wall specimens are shown in Fig. 4.3. The design of the HPFRC beams used at the first, third, and fourth levels accounts for the improved damage tolerance exhibited by HPFRC elements by assuming the full coupling beam section maintains its integrity and remains active in resisting shear and moment through large displacement reversals, reducing the need for diagonal and transverse reinforcement for resisting the applied shear. For comparison purposes, the second story beam in both specimens was cast with conventional concrete. The flexural and diagonal reinforcement were identical for the HPFRC and regular reinforced concrete (RC) coupling beams to provide similar flexural stiffness and strength. However, the transverse reinforcement ratio was increased from $\rho_t = 0.55\%$ for the HPFRC coupling beams to $\rho_t = 1.5\%$ in the reinforced concrete beams to provide additional shear resistance and confinement.

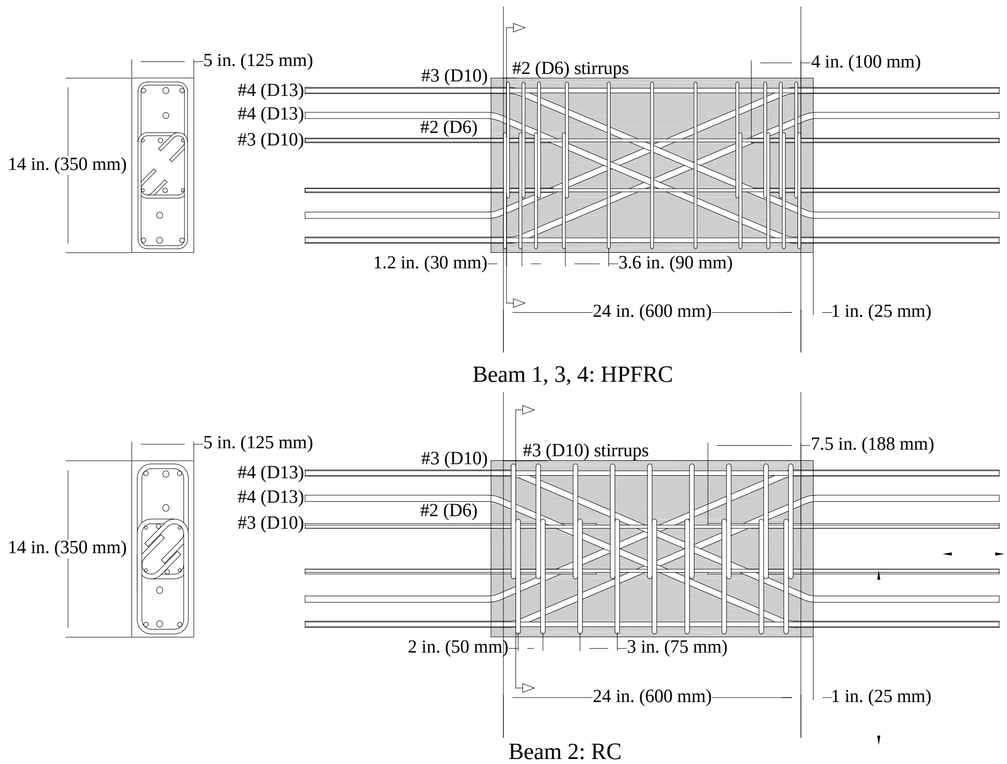

Beam 1, 3, 4: HPFRC

Beam 2: RC

Figure 4.3. Coupling beam reinforcement

4.2. Coupled Wall Design

The coupling beam dimensions and detailing were of special interest in this project, and thus, they were the initial focus of the coupled-wall system design. After the coupling beams, the structural walls of each specimen were designed to provide the required overturning moment capacity, shear strength, and ductility for the coupled-wall system to behave realistically (details shown in Fig. 4.4). In the first specimen, the walls were designed in accordance with the seismic provisions of the ACI Building Code (ACI 318-08). The second specimen incorporated fiber reinforcement in the first two stories of the system, providing increased shear resistance and allowing for reduced boundary element confinement. In the first specimen, the hoops confining the boundary element were spaced at the maximum spacing permitted by the ACI Building Code (ACI 318-08), of $b_w/3$. In the HPFRC specimen, hoops were spaced at $b_w/2$ on one wall and at b_w on the other.

The wall shear design was based on the expected ultimate capacity of the system, assuming that a mechanism controlled by flexural hinging at the base of both walls and in each of the beams would develop. To resist the expected shear demand, the wall concrete in the first coupled-wall system was assumed to carry a shear stress of $2\sqrt{f_c'},[psi](0.17\sqrt{f_c'},[MPa])$. Wall transverse (horizontal) reinforcement, anchored by alternating 90- and 135-degree hooks, was provided to resist the remaining shear, which resulted in a transverse reinforcement ratio of 0.45% in the reinforced concrete walls. The HPFRC used in the walls of the second test specimen was assumed to carry a shear stress of $4\sqrt{f_c'},[psi](0.33\sqrt{f_c'},[MPa])$.

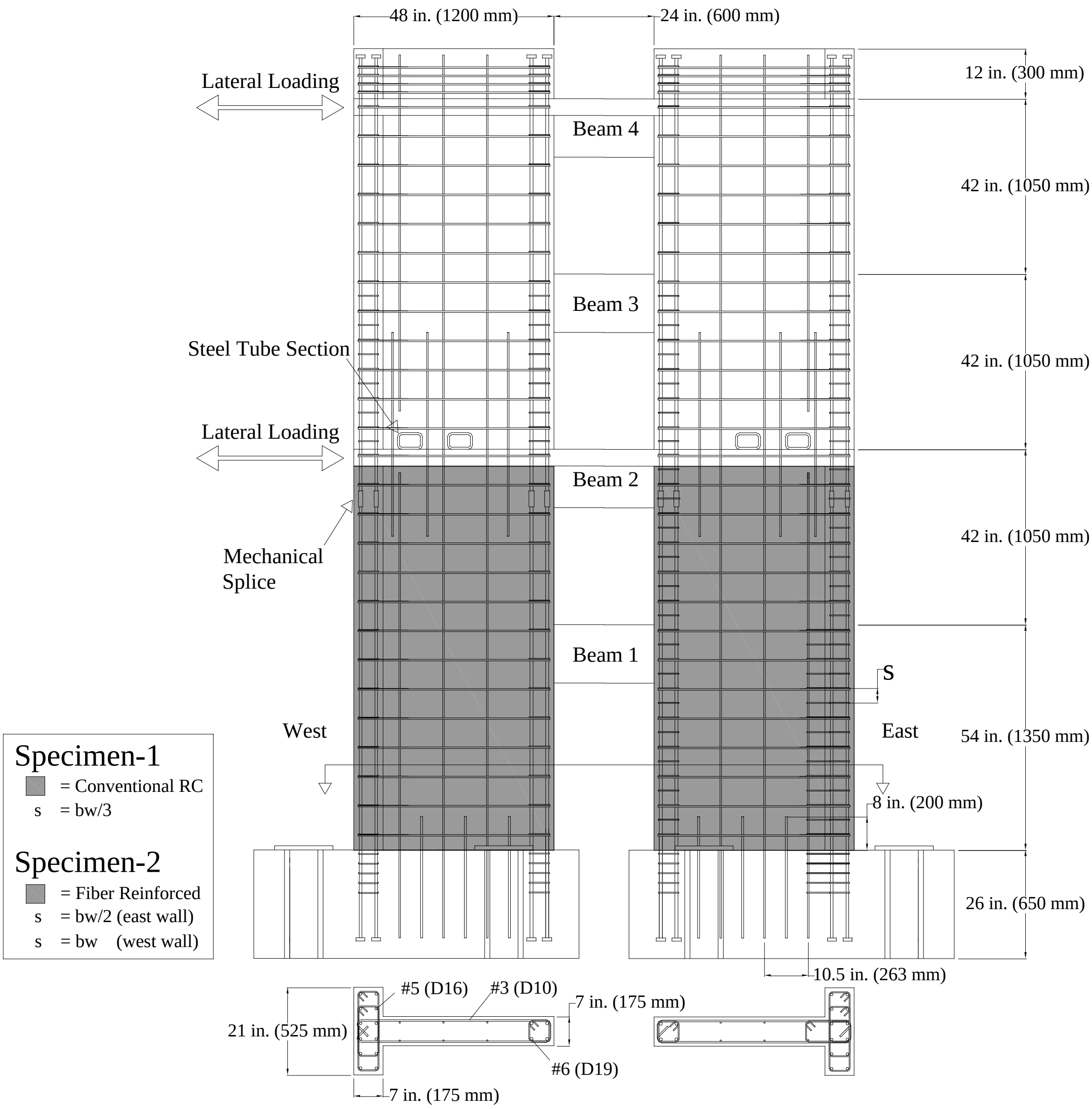

Figure 4.4. Coupled-wall system reinforcement

5. COUPLED-WALL TEST RESULTS

A plot of the overturning moment vs. drift responses for the two coupled-wall specimens is shown in Fig. 5.1. Both specimens exhibited the high strength and stiffness characteristic of coupled-walls, with excellent strength retention. The first specimen maintained more than 80% of the peak overturning moment capacity to beyond 2.5% drift in both loading directions. The second specimen exhibited higher drift capacity, retaining more than 80% of the peak strength to beyond 3% drift. Furthermore, the hysteresis loops show no appreciable pinching, because the responses were governed by flexural hinging in the bases of the walls and at the ends of the coupling beams, as intended in design.

5.1. Coupled Wall Cracking

The coupled walls exhibited predominantly diagonal-shear cracking at their base in early cycles, with flexural cracking becoming more prevalent at drifts beyond approximately 0.75%. This indicates that the ACI Building Code (ACI 318-08) requirements for structural wall design, and the proposed HPFRC design with reduced reinforcement, both provided adequate shear resistance and confinement of longitudinal reinforcement to accommodate a ductile flexural mechanism. Although the overall response of the HPFRC wall system was very similar to the companion RC specimen, the extent and severity of cracking differed. The HPFRC specimen exhibited a much higher number of narrower cracks when compared to the reinforced concrete wall system, as shown in Fig. 5.2. The HPFRC walls developed diagonal cracks spaced at approximately 2 in. (50 mm), less than half of the typical diagonal crack spacing of the first specimen. The individual crack widths were consistently less than half those observed in the RC specimen. This improved damage tolerance is typical of HPFRC members.

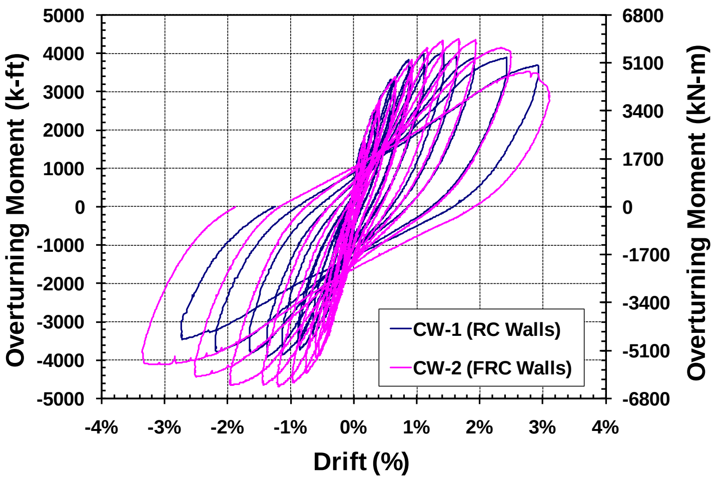

Figure 5.1. Overturning moment vs. drift for coupled-wall specimens

Figure 5.2. Structural-wall crack patterns near end of test (left: conventional concrete, right: HPFRC)

5.2. Coupling Beam Performance

For the purpose of comparing the behavior of the RC and HPFRC coupling beams, the performance of the second specimen will be highlighted. Diagonal-shear cracking was first observed in all four coupling beams near system drifts of 0.5%. At a system drift of 1.5%, initiation of spalling was first noted in the RC beam at the second level. When the system drift reached 2%, significant loss of cover had exposed much of the transverse reinforcement in the RC beam. The other beams, constructed with HPFRC, also began to exhibit wider cracks, but they remained less than 0.04 in. (1 mm) in width. It was not until the system had reached a drift of 2.5% that the HPFRC beams exhibited unsightly damage consisting of wider cracks and superficial flaking. However, at this same drift, the RC beam had spalled extensively, exposing nearly all of the reinforcement. Significant damage to the core of the RC coupling beam was evident. Fig. 5.3 shows a photo of the first two coupling beams at a system drift of 3.3% that illustrates the substantially greater damage tolerance exhibited by HPFRC beams.

5.2.1. Coupling beam chord rotations

For typical coupled-wall systems, the chord rotation expected in coupling beams (as defined in ASCE/SEI 41/06) can be roughly predicted as the inter-story wall rotation times the ratio of the distance between the wall centroidal axes to the effective length of the coupling beam (2.1 for the test specimens). The effective coupling beam length, L_{eff}, was defined as $L_{eff} = L + h$, where L is the clear span and h is the height of the beam (Wight and MacGregor 2009). The experimentally observed relationship between coupling beam chord rotations and inter-story wall rotations are shown in Fig. 5.4, plotted along with the predicted value. When the system drift reached 2.5%, nearly all of the coupling beams were subjected to chord rotations exceeding 4.0% (ratio = 1.6). Although these large deformation demands emphasize the need for highly ductile coupling beams, the observed ratio is lower than the calculated value of 2.1. This suggests that this rough predictor may regularly overestimate coupling beam chord rotation demands.

5.2.2. Coupling beam elongations

When reinforced concrete members are subjected to cyclic displacements large enough to cause significant cracking and yielding of the reinforcement, it is widely recognized that members have a tendency to expand longitudinally. In coupled-wall systems, the adjacent structural walls and surrounding slab may provide substantial resistance to this expansion, as identified by Teshigawara et al. (1998). Most experimental work on coupling beam components has allowed for unlimited axial elongation, which has been reported to be as high as 4.0% of the beam length (Kwan and Zhao 2002). Recent work (Lequesne et al. 2009) showed that appreciable axial forces develop within coupling beams when maximum average longitudinal strains are limited to between 0.5-1.0%. Fig. 5.5 shows the measured average axial strains of the coupling beams at all four stories at various inter-story drift levels. The magnitudes of the axial strain indicate significant restraint from the adjacent walls, and thus, the development of significant axial compression forces that will affect the capacity and ductility of the coupling beams.

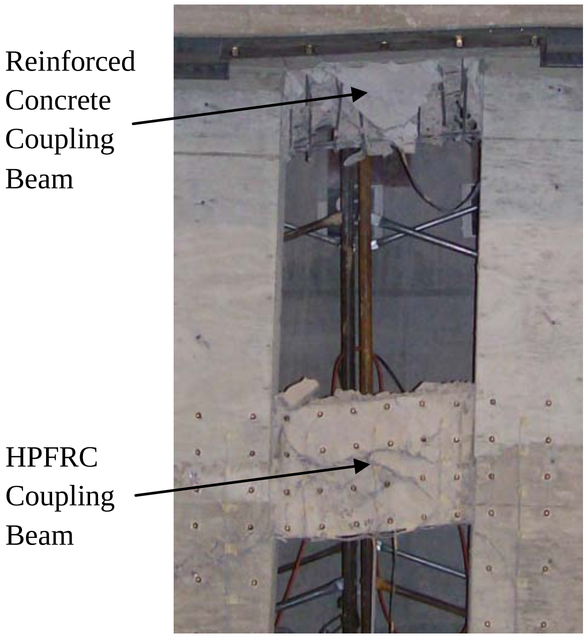

Figure 5.3. CW-2 beam damage

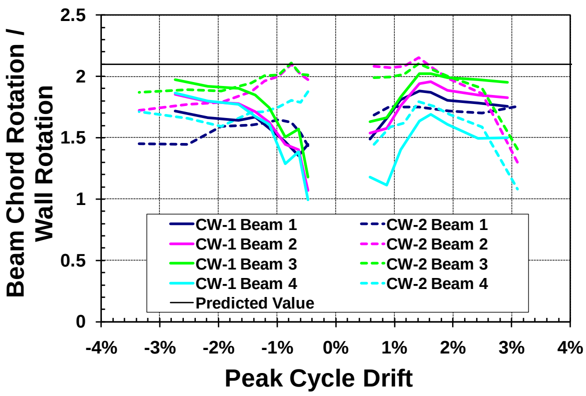

Figure 5.4. Coupling beam chord rotations

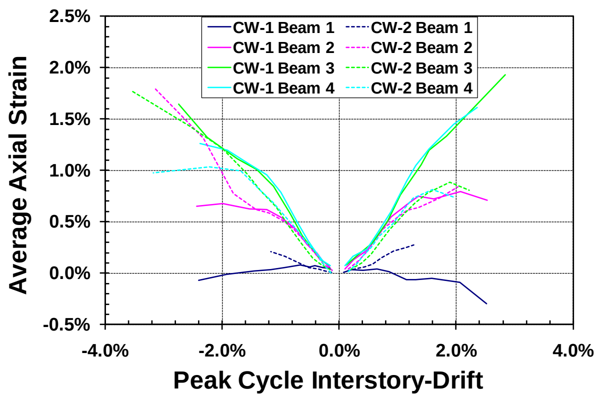

Figure 5.5. Coupling beam elongations

6. SUMMARY AND CONCLUSIONS

Two large-scale, four-story coupled-wall specimens were tested to investigate the impact that precast HPFRC coupling beams have on the design, construction, and behavior of coupled-wall systems. The design of the coupling beams was based on results from a series of coupling-beam-component tests that demonstrated the advantages, in terms of shear strength and ductility, of using HPFRC in coupling beams. HPFRC used in the wall plastic hinge regions allowed for a reduction of boundary element confinement and a higher shear stress contribution from the concrete in design. The following conclusions can be made regarding the performance of the systems tested.

- The coupled-wall specimens exhibited excellent strength retention up to system drifts as large as 3.0%. The HPFRC regions exhibited narrower crack spacing and improved damage tolerance, despite simplified reinforcement detailing.
- Spacing ties in the HPFRC wall boundary element at $b_w/2$ or b_w, as compared to $b_w/3$ for the RC walls, did not lead to premature failure in the HPFRC walls, indicating effective confinement was achieved.
- A design value of $4\sqrt{f_c'}, [psi](0.34\sqrt{f_c'}, [MPa])$ for the contribution of HPFRC to the nominal shear stress capacity of structural walls resulted in adequate resistance to shear.
- Coupling beam chord rotations, relative to inter-story wall rotations, were less than predicted. This implies that coupling beam chord rotations may be over-estimated by the traditional approach of amplifying beam rotations based on the ratio of the distance between the wall centroids and the coupling beam span.
- Measurements indicate the tendency for coupling beams to elongate when subjected to reversing displacements is substantially restrained by the adjacent structural walls and floor slabs. This translates into the development of significant axial forces that impact both the strength and ductility of coupling beams.
- Although not a focus of the current study, the ACI Building Code seismic requirements for structural wall design provided adequate shear resistance and confinement, which led to the development of a stable flexural mechanism.

ACKNOWLEDGEMENT
The tests reported were funded by the National Science Foundation through the NEES research program under Grant No. CMS 0530383 and Bekaert Corp. Special thanks also go to Erico Corp. for donation of materials used in construction of the specimens described. The ideas and conclusions are those of the writers and do not necessarily represent the views of the sponsors.

REFERENCES

ACI Committee 318 (2008), *Building Code Requirements for Structural Concrete (ACI 318-08) and Commentary*, American Concrete Institute, Farmington Hills, MI, 465 pp.

ASCE/SEI 41/06 (2007), *Seismic Rehabilitation of Existing Buildings*, American Society of Civil Engineers, Reston, Virginia.

ASTM C 1609/C 1609M – 05 (2005), "Standard Test Method for Flexural Performance of Fiber-Reinforced Concrete (Using Beam With Third-Point Loading)," West Conshohocken, PA.

Canbolat, B. A., Parra-Montesinos, G. J., and Wight, J. K. (2005), "Experimental Study on Seismic Behavior of High-Performance Fiber-Reinforced Cement Composite Coupling Beams," *ACI Structural Journal*, V. 102, No. 1, pp. 159-166.

Kwan, A. K. H., and Zhao, Z. Z. (2002), "Cyclic Behaviour of Deep Reinforced Concrete Coupling Beams." *Structures and Buildings*, V. 152, No. 3, pp. 283-293.

Lequesne, R. D., Setkit, M., Parra-Montesinos, G. J. and Wight, J. K. (2009), "Seismic Detailing and Behavior of Coupling Beams With High-Performance Fiber Reinforced Concrete," *Antoine E. Naaman Symposium – Four decades of progress in prestressed concrete, fiber reinforced concrete, and thin laminate composites*, SP-XX, American Concrete Institute, Farmington Hills, MI, 14 pp, In Press.

Liao, W. C., Chao, S. H., Park, S. Y. and Naaman, A. E. (2006), "Self-Consolidating High Performance Fiber Reinforced Concrete (SCHPFRC) – Preliminary Investigation," *Report No. UMCEE 06-02*, University of Michigan, Ann Arbor, MI, 68 pp.

Teshigawara, M., Kato, M., Sugaya, K. and Matsushima, Y. (1998), "Energy Absorption Mechanism and the Fluctuation of Shear Force in the Coupled Shear Walls," *Structural Engineers World Congress 1998*, Paper Number T-186-5, Elsevier Science Ltd.

Wight, J. K.; and MacGregor, J. G. (2009), *Reinforced Concrete: Mechanics and Design*. 5th ed. Upper Saddle River, New Jersey, pp 1112.